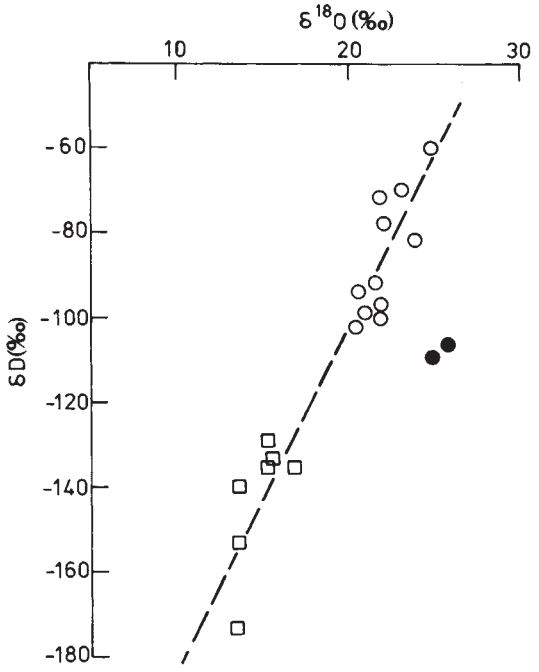

Fig. 2 Plot of δD (relative to V-SMOW) of H_2O^+ against silicate $\delta^{18}O$ (relative to V-SMOW) for Scottish agates. The circles are Lower Devonian samples, with filled symbols for JJ12 and JJ17 (see text). The squares are Tertiary samples. The dotted line is $\delta D = 8.4\delta^{18}O - 271$, the best-fit line through the 11 open circles, shown extrapolated to the region of the Tertiary data.

may be significant that six points plot low, close together at ~(+21‰, −98‰); these could represent a pure meteoric water endmember. Assuming this and adopting 60‰ for the δD fractionation, Lower Devonian waters would be ~(−5‰, −30‰).

The high $\delta^{18}O$, low δD samples JJ12 and JJ17 are problematic. We speculate that for some, as yet unknown, reason they formed at a lower temperature than the others. Assuming that the same formation waters were involved, the $\delta^{18}O$ shift implies a temperature of 30 °C (Knauth-Epstein[10] calibration) or 50 °C (Clayton *et al.*[16] calibration). The agate/water δD fractionation of 80‰ would then correspond approximately to a rate of change of 20‰ in 16 °C or ~1.3‰ °C^{-1}. This is the same as the value derived from ref. 15 and so the argument is at least consistent. Contrary to previous discussions[1,2,6,8], our work strongly supports a low-temperature genesis for agates, and similar temperature estimates for the majority of Lower Devonian and Tertiary agates are a necessary consequence of our interpretation of the data distribution as representing a co-linear trend parallel to a common meteoric water line.

Returning to the idea of agates as 'refused' marine chert xenoliths, we note that δD of deep-sea cherts is not a function of $\delta^{18}O$ (ref. 11). Also, the data in Fig. 2 show convincingly for the Scottish samples that meteoric water had a role in establishing the isotopic compositions. May the arguments[2] be relaxed, then, to allow some agates to be refused freshwater cherts (see ref. 17)? This seems unlikely. The investigation[9] of nodular and bedded cherts suggested $\delta D = 8\delta^{18}O - 328$ for Tertiary samples and $\delta D = 8\delta^{18}O - 279$ for Devonian samples from continental North America, yet a notable feature of the data in Fig. 2 is that a single line is defined for both Devonian and Tertiary agates, the majority of points plotting close to $\delta D = 7.9\delta^{18}O - 260$. Tectonic difficulties associated with the xenolithic idea are exacerbated by the complication that although $\delta^{18}O$ of deep-sea cherts might not be finally established until ~10 Myr after deposition[11], the agates found in Scottish Tertiary lavas appear to have interacted with highly depleted—and by implication Tertiary—waters during formation.

The relationship between $\delta^{18}O$ of microcrystalline quartz and δD of bound water implies that formation fluid has been retained. Models of agate genesis that appear to involve sequences of fluids[1,18] can now be tested isotopically. For other agate suites, like those discussed here, it is possible to estimate the isotopic composition of the local meteoric water during past geological times.

We thank those who donated agates, especially Graham Durant, Colin Currie, G. Scowen, B. Jackson, W. J. Baird and H. Macpherson. We also thank I. M. Mills, J. F. Hewitt, J. Bennet and D. MacLean for preparing the manuscript; P. J. Hamilton and other colleagues in the Isotope Geology Unit for useful discussions; Professor M. J. Russell (Strathclyde Univ.) for support for C.B. Stable isotope work at SURRC is supported by NERC and the Scottish Universities. A.E.F. thanks Mr A. V. Caira for invaluable help.

Received 8 October; accepted 20 September 1984.

1. Florke, O. W., Kohler-Herbertz, B., Langer, K. & Tonges, I. *Contr. Miner. Petrol.* **80**, 324-333 (1982).
2. Blankenburg, H.-J., Pilot, J. & Werner, C.-D. *Chem. Erde* **41**, 213-217 (1982).
3. Blankenburg, H.-J., Werner, C.-D., Schron, W. & Klemm, W. *Z. geol. Wiss.* **10**, 1287-1298 (1982).
4. Braitsch, O. *Heidelb. Beitr. Miner. Petrogr.* **5**, 331-372 (1957).
5. Frondel, C. *The System of Mineralogy* (Vol. III) *Silica Minerals* (Wiley, London, 1962).
6. Blankenburg, H.-J. & Berger, H. *Chem. Erde* **40**, 139-145 (1981).
7. Blankenburg, H.-J., Schron, W., Starke, R. & Klemm, W. *Chem. Erde* **42**, 157-172 (1983).
8. Blankenburg, H.-J. *Jena Rev.* **2**, 68-70 (1983).
9. Knauth, L. P. & Epstein, S. *Geochim. cosmochim. Acta* **40**, 1095-1108 (1976).
10. Knauth, L. P. & Epstein, S. *Earth planet. Sci. Lett.* **25**, 1-10 (1975).
11. Kolodny, Y. & Epstein, S. *Geochim. cosmochim. Acta* **40**, 1195-1209 (1976).
12. Taylor, H. P. & Forester, R. W. *J. Petrol.* **12**, 465-497 (1971).
13. Forester, R. W. & Taylor, H. P. *Earth planet. Sci. Lett.* **32**, 11-17 (1976).
14. Forester, R. W. & Taylor, H. P. *Am. J. Sci.* **277**, 136-177 (1977).
15. Savin, S. M. in *Handbook of Environmental Isotope Geochemistry* Vol. 1 (eds Fritz, P. & Fontes, J. Ch.) 283-327 (Elsevier, Amsterdam, 1980).
16. Clayton, R. N., O'Neil, J. R. & Mayeda, T. K. *J. geophys. Res.* **77**, 3057-3067 (1972).
17. Knauth, L. P. *Geology* **7**, 274-277 (1979).
18. Sunagawa, I. & Ohta, E. *Sci. Rep. Tohuku Univ.* **13**, 131-146 (1976).

Redistribution of fallout radionuclides in Enewetak Atoll lagoon sediments by callianassid bioturbation

Gary M. McMurtry*, Randi C. Schneider*, Patrick L. Colin†‖, Robert W. Buddemeier‡ & Thomas H. Suchanek§‖

* Hawaii Institute of Geophysics, University of Hawaii, Honolulu, Hawaii 96822, USA
† Mid-Pacific Research Laboratory, Enewetak Atoll, Marshall Islands, c/o Hawaii Institute of Marine Biology, University of Hawaii, Kaneohe, Hawaii 96744, USA
‡ Lawrence Livermore Laboratory, University of California, Livermore, California 94550, USA
§ West Indies Laboratory, Fairleigh Dickinson University, Tague Bay, Christiansted, St Croix, US Virgin Islands 00820, USA

The lagoon sediments of Enewetak Atoll in the Marshall Islands contain a large selection of fallout radionuclides as a result of 43 nuclear weapon tests conducted there between 1948 and 1958 (refs 1, 2). Studies of the burial of fallout radionuclides have been conducted on the islands[3,4] and in several of the large craters[1,5], but studies of their vertical distribution have been limited to about the upper 20 cm of the lagoon sediments. We have found elevated fallout radionuclide concentrations buried more deeply in the lagoon sediments and evidence of burrowing into the sediment by several species of callianassid ghost shrimp (Crustacea: Thalassinidea) which has displaced highly radioactive sediment. The burrowing activities of callianassids, which are ubiquitous on the lagoon floor, facilitate radionuclide redistribution and complicate the fallout radionuclide inventory of the lagoon.

The Enewetak radiological survey of 1972 (ref. 1) extensively sampled the surface sediment of the atoll lagoon and identified

‖ Present addresses: Motupore Island Research Department, University of Papua New Guinea, Box 320, University, Papua New Guinea (P.L.C.); Division of Environmental Studies, University of California, Davis, California 95616, USA (T.H.S.).

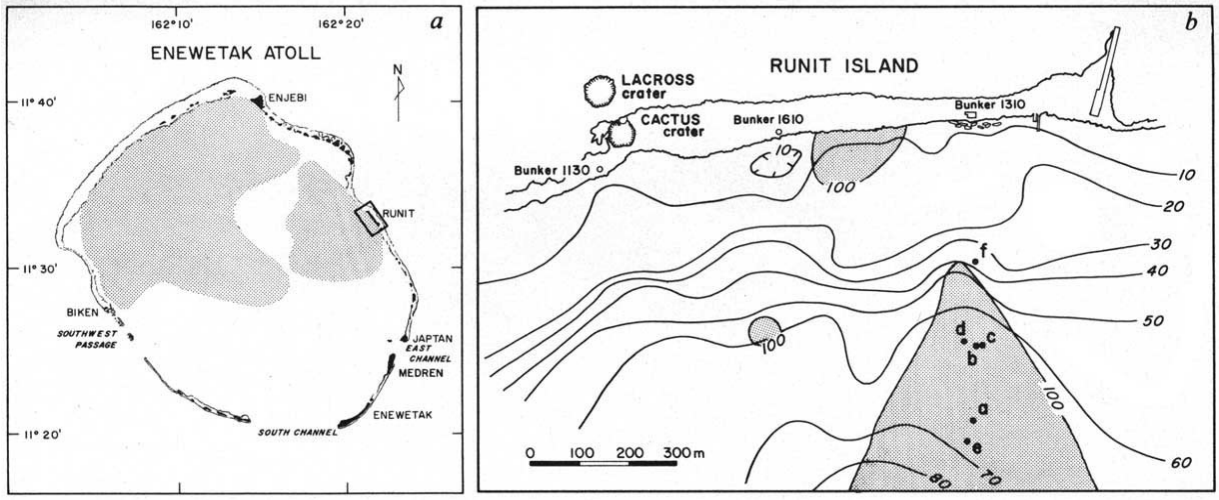

Fig. 1 *a*, Location map of Enewetak Atoll, Marshall Islands. Shaded areas are surficial lagoon sediments with >100 mCi km^{-2} $^{239+240}Pu$. Box indicates location of detailed study area off Runit Island (after ref. 1). *b*, Detailed study area showing sample locations a–f (G.M.M. *et al.*, unpublished data). Shaded areas are surficial lagoon sediments with >100 pCi g^{-1} $^{239+240}Pu$. Bathymetric contours in feet (after ref. 1).

two areas having significant contamination: the north-west lagoon extending south-west of Enjebi and a smaller area extending south-west of Runit (Fig. 1*a*). Because these sediments contain most of the atoll radionuclide inventory and possess an active, burrowing infauna, we investigated the vertical distribution of fallout radionuclides in a series of cores taken by SCUBA divers within the contaminated area south-west of Runit Island (Fig. 1*b*).

Eleven sediment cores between 20 and 200 cm in length were recovered from an area of the lagoon floor suspected to contain the fallout contamination of several nuclear detonations on floating barges (Fig. 1*b*). The cores were recovered by hammering 3-inch diameter plastic core liners into the sediment, which were capped and extracted. Six of these cores exhibit large amounts of radioactivity in distinct layers as identified by γ spectrometry, α spectrometry, and α and β autoradiographic techniques. Two of these cores, 5C-1 and 5D-3 (sites c and d in Fig. 1*b*), were singled out for the present detailed analyses because: (1) they contained unusually large amounts of radioactivity associated with a thick distinct layer of fine-grained carbonate material and (2) they readily displayed the effects of bioturbation. A more comprehensive report on these sediments will appear elsewhere (G.M.M. *et al.*, unpublished data).

The lagoon sediments are primarily composed of an unconsolidated mixture of the skeletal remains of corals, coralline algae (*Halimeda* sp.), and foraminifera[6]. The lagoon floor in the sampling area is populated by scattered *Halimeda* colonies and ubiquitous mounds of reworked sediment and associated 'sink holes' produced by populations of several species of burrowing callianassid ghost shrimp (Crustacea: Thalassinidea). At least four different species have been identified, each in a separate genus and all from the family Callianassidae (*Callianassa* sp., *Calliax* aff. *C. novaebritanniae* (Borradaile), *Callichirus vigilax* (de Man) and *Thomassinia* sp.). Numerous other invertebrates and fishes at Enewetak contribute to bioturbation of lagoon sediments, but callianassid shrimps seem to have the greatest impact on sediment redistribution. During feeding and tunnel construction these callianassids often burrow to depths of >1.5 m below the sediment surface and sort through massive quantities of sediment to glean organic material[7]. Coarse-grained sediments (≥1.4 mm) are stored in subsurface refuse galleries. Smaller particles are either used in burrow wall construction or pumped to the sediment–water interface where they are either suspended in the water column or accumulate in the form of mounds[7,8]. The two cores described here were taken 60 m apart among dense callianassid mounds; both cores display evidence of callianassid burrowing (Figs 2 and 3).

The sediment cores were split lengthwise into two halves. One-half was surveyed by a scanning γ-spectrometer system equipped with a NaI(Tl) detector. The remaining half was surveyed by α and β autoradiography. α-Sensitive, Kodak LR-115 cellulose nitrate film was placed directly on the core for 2 months and developed as described in ref. 9. α Tracks were counted by a random field-of-view method with a light microscope. To assess total β activity, Kodak AA-2 Industrial X-ray film was placed on the core half for 4 months. A 0.01 mm thick plastic sheet was placed between the core and X-ray film to prevent chemical reactions and α-particle exposure. High-energy γ rays are too energetic to expose this film. The films were scanned with a densitometer and generated density plots

Table 1 Radionuclide concentrations in Enewetak Lagoon sediments off Runit Island (pCi g^{-1})

Core no.	Depth (cm)	^{60}Co	^{125}Sb	^{137}Cs	^{152}Eu	^{154}Eu	^{155}Eu	^{207}Bi	^{226}Ra	^{238}Pu	$^{239+240}Pu$	^{241}Am
5C-1	0–5	35±1	1.6±0.2	11.1±0.3	0.7±0.1	0.3±0.1	35±1	0.6±0.1	0.1†	(12±2)	(130±20)	19±1
	0–5*	23±1	0.9±0.1	8.2±0.1	0.7±0.1	0.1	30±1	0.5±0.1	0.1†	8.6±0.1	101±1	17±2
	5–9	28±1	1.4±0.1	10.1±0.2	0.5±0.1	0.3±0.1	27±1	0.5±0.1	0.1†	9.4±0.1	108±1	15±2
	48–53	445±4	46±1	101±2	2.3±0.5	0.6	132±2	0.2	0.4†	(6±1)	(63±9)	9±1
	133–138	35±1	3.6±0.2	59±1	0.1	0.2	13.1±0.3	0.1	0.1†	(0.7±0.1)	(8±1)	1.2±0.3
5D-3	0–5	14±1	0.5±0.1	2.1±0.1	0.4±0.1	0.1	21.5±0.4	1.6±0.1	0.1†	(14±2)	(150±20)	22±1
	5–8	11.9±0.1	0.5±0.1	1.9±0.1	0.4±0.1	0.1	19.4±0.3	1.4±0.1	0.3±0.1	12.5±0.1	114±1	19±1
	32–36	47±1	3.5±0.2	3.7±0.2	0.5±0.1	0.4±0.1	30±1	3.7±0.1	0.4±0.1	26.7±0.3	295±3	37±2
	61.5–66.5	1424±7	149±1	166±3	8±1	4.2±0.7	405±8	0.4	0.6†	(36±5)	(360±50)	55±5
	109–113	62±2	5.4±0.2	5.4±0.2	0.6±0.1	0.2	21.7±0.4	0.1	0.1†	(1.0±0.1)	(11±1)	1.6±0.4

Analyses performed at Lawrence Livermore Laboratory by γ spectrometry using a Ge(Li) detector except Pu analyses by α spectrometry. Errors are based on counting statistics ($\pm 1\sigma$). Bracketed Pu values are estimated from mean Pu/Am isotope ratios.

* Replicate analysis based on adjacent sample of core. All analyses reported as of 5 March 1982.

† Upper limit values only.

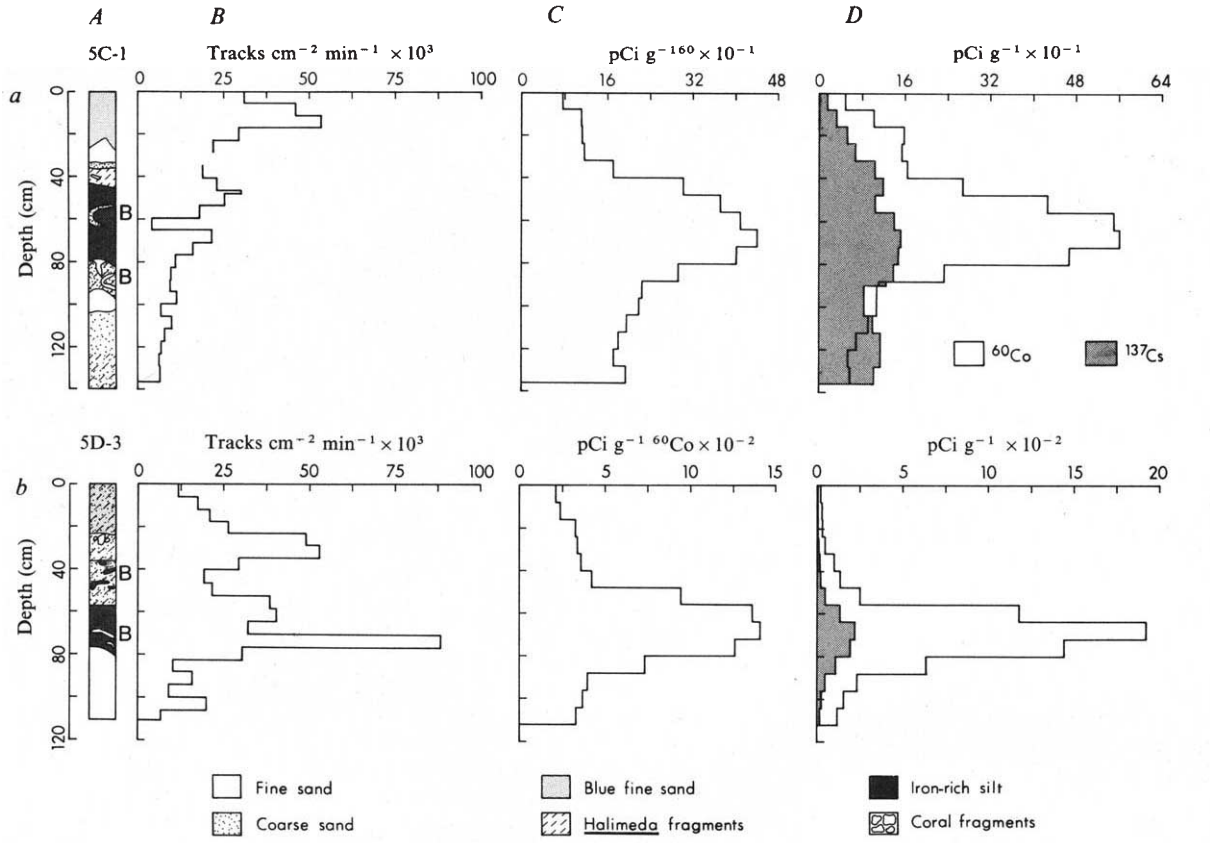

Fig. 2 Detailed vertical radioactivity distributions in cores Runit 5C-1 (*a*) and 5D-3 (*b*). *A*, General lithological descriptions of sediment cores. Major areas of burrows are indicated by 'B'. *B*, Total α-activity distribution. *C*, Total β-activity distribution as ^{60}Co. *D*, Distribution of ^{60}Co and ^{137}Cs.

were integrated by using a polar planimeter. Total β activities were standardized with a ^{60}Co source designed to approximate the self-absorption of the cores.

Selected samples of the cores were analysed by α and γ spectrometry at Lawrence Livermore Laboratory. Samples for γ analysis were dried and coarsely ground before counting on a Ge(Li) spectrometer system. Splits of these samples were dissolved in concentrated acids and Pu was preconcentrated by anion exchange before α spectrometry using Si(Li) detectors.

These sediments contain a complex assemblage of nuclear fuel, fission and activation products and their decay products[1,2]. The abundance of many of the long-lived radionuclides that contribute to the α, β and γ activity are presented for selected sections of the cores in Table 1. Detailed vertical radioactivity distributions of total α, total β, and the major β and γ-emitting isotopes ^{60}Co and ^{137}Cs are shown in Fig. 2.

Both cores contain discrete layers of predominantly fine-grained (<38 μm) carbonate material which correspond to peaks in radioactivity at depths of 43–80 cm and 56–88 cm, respectively, for cores 5C-1 and 5D-3 (Fig. 2). This fine-grained carbonate is probably blast-pulverized sediment and reef material formed by cratering from nearby barge events. After an almost instantaneous deposition of the fine-grained carbonate layer, deposition of predominantly coarser-grained sediments occurred by either slumping, normal sedimentation or some combination of these processes (Fig. 2). Similar fine-grained sediments have been observed in and adjacent to the Enewetak nuclear craters on land[5]. These barge events occurred during the Hardtack Phase I Series from May to August of 1958, the last series of tests conducted at Runit[2].

Chemical, mineralogical and scanning electron microscopy–energy dispersive X-ray analysis (SEM–EDAX) of carbonate dissolution residues reveal that these fine carbonate layers contain 1–2 wt % non-carbonate material composed largely of magnetite with minor amounts of pyrite and amorphous biogenic silica. This noncarbonate material contains >90% of the total radioactivity in the sample.

Adams *et al.*[10] found that fallout particles collected following nuclear weapons detonations at Enewetak were formed by the interaction of condensing vaporized metals and fission products from the bomb and associated structures with surface material swept up into the cooling fireball. In the case of barge events, these particles were largely small (<1-μm) spheres of dicalcium ferrite formed from the condensation of the vaporized barge and ballast materials; magnetite and calcium oxide were identified as major components of fallout particles from tower and ground shots on land[10].

Probably most, if not all, of the radioactivity in these sediments was originally present in the magnetite. SEM–EDAX results indicate that the pyrite has formed *in situ* by postdepositional interaction of dissolved Fe^{2+} and sulphide derived from bacterially mediated reduction of porewater sulphate in anoxic conditions[11]. Inspection of the fine-grained carbonate layers both immediately after collection of the cores and after splitting revealed black and greyish-brown colours for 5D-3 and 5C-1, respectively, indicating that core 5C-1 was oxidized relative to 5D-3. X-ray diffraction analysis of the noncarbonate fraction of both cores indicates the presence of X-ray amorphous material in the 5C-1 layer that may be iron (III) oxide; chemical analysis of both fractions rule out the possibility that this amorphous material is composed of a greater amount of biogenic silica.

Because of their similar lithological, chemical, mineralogical, and radionuclide compositions, it seems likely that the two closely spaced cores have sampled either the same radioactive layer or layers produced by closely spaced tests of similar effect. Visual observation of both cores suggests that core 5C-1 is more heavily bioturbated than 5D-3. Even in core 5D-3, β autoradiography reveals that burrowing into the fine carbonate layer has displaced highly radioactive material and replaced it with less radioactive coarser-grained material from layers above

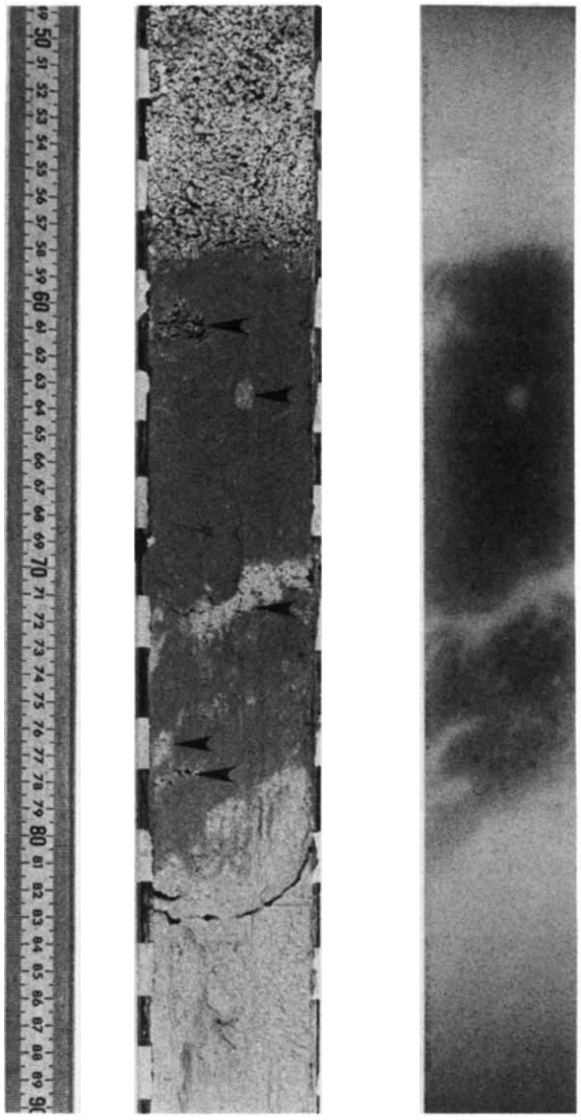

Fig. 3 Iron-rich, carbonate silt layer in core 5D-3. Callianassid burrows are indicated by arrowheads. β autoradiograph (right) shows callianassid burrows filled with less radioactive sediment from adjacent layers (light tones). Dark tones indicate highly radioactive sediment.

and below the fine carbonate (Fig. 3). The fine carbonate layer of core 5C-1 contains about one-third of the iron content and overall radioactivity of core 5D-3 (Table 1 and Fig. 2). Comparison of grain-size distributions in samples taken from these layers where no major burrows are evident suggests that the 5C-1 layer also contains a greater amount of coarser-grained carbonate material.

These observations suggest greater mixing of less-radioactive material into or greater transport of more-radioactive material out of the 5C-1 fine carbonate layer, or both. Callianassid burrowing could easily account for any combination of these sediment transport processes. The relative degree of burrowing into these layers may also be reflected by their relative degree of oxidation. For at least the absolute concentrations, however, we cannot rule out core-to-core variations over small distances due to such factors as variable deposition or even variable test yield should the cores have sampled different blast areas. Indeed, the different radionuclide ratios in the fine-grained carbonate layers of the two cores, if unaffected by the bioturbation, strongly suggest that they have received debris from different tests (Table 1).

The distributions of ^{60}Co, ^{137}Cs and transuranic activities suggest either different deposition or redistribution of transuranic isotopes relative to that of ^{60}Co in both cores and of ^{137}Cs relative to ^{60}Co in core 5C-1 (Table 1 and Fig. 2). Redistribution, by callianassid activity or another process, assumes that most of the radioactivity observed in the two cores originated in the fine carbonate layers and that no significant radioactive deposition occurred in the area before or after the deposition event. It is unfortunate that, given the complex history of testing at Enewetak Atoll and, in particular, the lagoon area off Runit Island[1,2], deposition of ^{137}Cs and transuranic isotopes before and after those deposited in the fine carbonate layers cannot be excluded.

Our findings have implications for both the atoll radionuclide inventory and for the mobilization of this inventory in the sediments and bottom waters of the lagoon. Previous estimates of the inventory identified the lagoon sediments as the largest reservoir, but relied on samples within the topmost 20 cm of the sediment column[1,12]. These estimates are certainly minimum values. Although our samples are from a small portion of the lagoon where burial of radionuclides may only be associated with cratering, it is precisely those areas where the levels of contamination are greatest[1]. If we use this area to extrapolate the lagoon sediment radionuclide inventory, previous estimates are 3–10 times too low. Further, a significant portion of the initial surface fallout deposition to the entire lagoon floor may be mixed to depths of at least 1.5 m by callianassid activity. Burial of fallout radionuclides by the bioturbation of unspecified benthic burrowing organisms is often invoked to explain the vertical distribution of these radionuclides in the topmost 10–30 cm of marine sediments[13–15], and the vigour and scale of burrowing activity in the marine environment has become more widely recognized[7,8,16–20]. Callianassids are found at all water depths within the lagoon; the mean number of large ($\geq$5 cm diameter) mounds increases from 1 m^{-2} at 15–30 m to 2.5 m^{-2} below 30 m and sometimes exceeds 7 m^{-2}. Deep-sediment mixing by callianassids would, therefore, add to the underestimation of lagoon sediment radionuclide inventories based on values determined from surface samples taken 14 yr after the testing period. Where fallout radionuclides have been deeply buried, the burrowing abilities of callianassids may recycle radionuclides to the sediment–water interface where dispersion into the overlying water column would be enhanced.

We thank Terry Kerby of the National Undersea Research Program at the University of Hawaii, Hawaii Undersea Research Laboratory and the staff of the Mid-Pacific Research Laboratory for field technical assistance. We also thank Sally Wickramaratne for laboratory assistance. This study was supported by the US Department of Energy under contract no. DE-AT03-81EV10699 (G.M.M.) and contract DE-AC08-76EV00703 for operation of the Mid-Pacific Research Laboratory. Hawaii Institute of Geophysics contribution no. 1570.

Received 25 July; accepted 3 December 1984.

1. US Atomic Energy Commission, *Enewetak Radiological Survey* NVO-140, Vol. 1 (Nevada Operations Office, Las Vegas, 1973).
2. US Department of Energy, *Enewetak Radiological Support Project* NVO-213, Final Rep. (Nevada Operations Office, Las Vegas, 1982).
3. Gudiksen, P. H. & Lynch, O. D. T. Jr *Health Phys.* **29**, 17–25 (1975).
4. Bliss, W. (compiler), *Enewetak Fact Book* (US Department of Energy, Nevada Operations Office, Las Vegas, 1982).
5. Ristvet, B. L. *Geological and Geophysical Investigations of the Eniwetok Nuclear Craters* AFWL-TR-77-242 (Air Force Weapons Laboratory, Air Force Systems Command, Kirtland AFB, 1978).
6. Emery, K. O., Tracy, J. I. Jr & Ladd, H. S. *Geol. Surv. Prof. Pap.* 260-A (1954).
7. Suchanek, T. H. *J. mar. Res.* **41**, 281–298 (1983).
8. Roberts, H. H., Suchanek, T. H. & Wiseman, W. J. *Proc. 4th int. Coral Reef Symp.*, Manila, **1**, 459–465 (1982).
9. Buddemeier, R. W., Biermann, A. H. & Gatrousis, C. *Lawrence Livermore Laboratory Rep.* UCRL-80679 (1978).
10. Adams, C. E., Farlow, N. H. & Schell, W. R. *Geochim. cosmochim. Acta* **18**, 42–56 (1960).
11. Berner, R. A. *Am. J. Sci.* **268**, 1–23 (1970).
12. Noshkin, V. E. in *Transuranic Elements in the Environment* (ed. Hanson, W. C.) 578–601 (US Department of Energy, Washington DC, 1980).
13. Peng, T.-H., Broecker, W. S., Kipphut, G. & Shackleton, N. in *The Fate of Fossil Fuel CO_2 in the Oceans* (eds Anderson, N. R. & Malahoff, A.) 355–373 (Plenum, New York, 1977).
14. Livingston, H. D. & Bowen, V. T. *Earth planet. Sci. Lett.* **43**, 29–45 (1979).
15. Santschi, P. H. *et al. Geochim. cosmochim. Acta* **47**, 201–210 (1983).
16. Shinn, E. A. *J. Paleont.* **42**, 879–894 (1968).
17. Ott, J. A., Fuchs, B., Fuchs, R. & Malasek, A. *Senckenbergiana Maritima* **8**, 61–79 (1976).
18. Pemberton, G. S., Risk, M. J. & Buckely, D. E. *Science* **192**, 790–791 (1976).
19. Weaver, P. P. E. & Schultheiss, P. J. *Nature* **301**, 329–331 (1983).
20. Kershaw, P. J., Swift, D. J., Pentreath, R. J. & Lovett, M. B. *Nature* **306**, 774–775 (1983).